SINGLE IMAGE DEHAZING WITH IMAGE ENTROPY AND INFORMATION FIDELITY

Dubok Park[1], Hyungjo Park[3], David K. Han[2], Hanseok Ko[3]

[1]Dept. of Visual Information Processing, Korea University, Seoul, Korea
[2]Ocean Engineering and Marine Systems Team, Office of Naval Research, Arlington, VA, USA
[3]School of Electrical Engineering, Korea University, Seoul, Korea

ABSTRACT

In this paper, we propose a new single image dehazing approach based on information fidelity and image entropy. The global atmospheric light is estimated by quad-tree subdivision using transformed hazy images. Then, transmission is estimated by an objective function which is comprised of information fidelity and image entropy at non-overlapped sub-block regions. This is further refined by a Weighted Least Squares (WLS) optimization procedure to alleviate block artifacts. We compared performance of the proposed method with conventional methods to validate its effectiveness in an experiment.

Index Terms— Airlight, dehazing, image entropy, edge-preserving smoothing, transmission

1. INTRODUCTION

Images of outdoor scenes are often degraded by turbid medium, such as dirt particles and water droplets, in the atmosphere. Light is scattered or attenuated as it travels through these particles, resulting less image radiance reaching the imaging sensor. Scene information is further corrupted by so called the "airlight" originated from ambient light reaching the sensor by the scattering medium [1]-[4]. It can be said that the image degradation due to airlight and the attenuated light from the scene is directly linked to the distance from the scene to the imaging sensor. Image degradation extends to scene color content since light attenuation through a turbid medium is not spectrally uniform.

There have been a number of techniques developed for haze removal to enhance scene visibility and restore color content [5]-[13]. Recently, there are single image haze removal methods due to the practical real-world applications [6, 7, 8, 9, 23]. Fattal et al. proposed a single image dehazing method using albedo of a scene [6]. Their method estimated the transmitted object radiance using statistical independence between shading and albedo. However, it requires adequate color information and its performance greatly depends on the statistical information of a hazy image. Tan et al. proposed a hazy image enhancement method using chromaticity [7]. However, this method can occasionally result oversaturated colors because maximizing contrast using the number of edges tends to overestimate the haze layer. K. He et al. restored a hazy image using the Dark Channel Prior (DCP) which is derived from statistics of haze-free images [8]. However, their method dose not sometimes remove a haze effectively since some images may not coincide derived statistics. They also refined transmission with an alpha matting to reduce the block artifacts. However, their method requires heavy computational load. J. Kim et al. proposed a haze removal method based on contrast enhancement [9]. They estimated transmission by minimizing a cost function which consists of uniformness of the histogram and the standard deviation. However, their method sometimes results in color distortion or over-stretched artifacts if there are many truncation pixels when calculating the cost function.

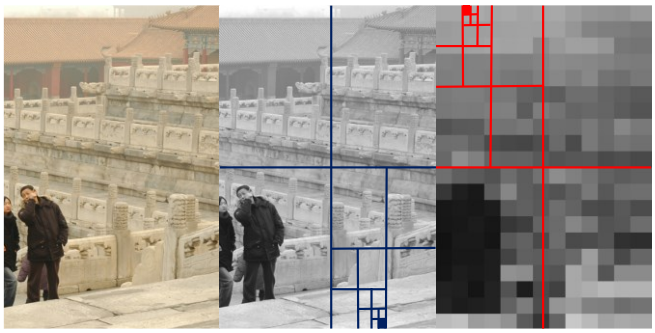

(a) (b) (c)

Fig. 1. Atmospheric light estimation. (a) Hazy image. (b) Conventional method [9]. (c) Proposed method. The blocks filled with blue and red color are the finally selected region.

To remove haze effectively those artifacts in the conventional method, we present a single image dehazing method based on an objective function which consists of image entropy and information fidelity. This paper is organized as follows. In Section 2, we describe the atmospheric scattering model. Section 3 describes detailed description of the proposed method. Section 4 provides a performance comparison with conventional methods. Finally, we deliver our conclusion in Section 5.

2. HAZY IMAGE MODELING

Generally, the exact nature of scattering is highly complex and depends on the types, size, orientation and distributions of particles constituting the media as well as wavelengths, polarization states and direction of the incident light [11]-[15].

The observed color of images captured under hazy condition can be modeled, based on the atmospheric optics [8, 9],

$$\mathbf{I}(\mathbf{x}) = \mathbf{J}(\mathbf{x})r(\mathbf{x}) + \mathbf{A}(1 - r(\mathbf{x})), \tag{1}$$

where, $\mathbf{x}$ is a spatial location in the image, $\mathbf{I}$ is the observed intensity, $\mathbf{J}$ is the scene radiance, $\mathbf{A}$ is the atmospheric light which

This research was supported by Seoul R&BD Program(WR080951)

(a) (b) (c)

Fig. 2. (a) Hazy image. (b) Dehazed result using estimated transmission without $f_{fidelity}$. (c) Dehazed result using estimated transmission with $f_{fidelity}$.

is assumed to be globally constant. r is the medium transmission describing the portion of the light that is not scattered and reaches the camera. From (1), the total irradiance is usually described by the sum of the direct attenuated irradiance $\mathbf{J}(\mathbf{x})r(\mathbf{x})$ and the airlight irradiance $\mathbf{A}(1 - r(\mathbf{x}))$. As the transmission r decreases, the airlight accumulates and becomes more intense in the hazy images. Essentially, the goal of single image haze removal is to recover $\mathbf{J}$ from (1) rewritten as

$$\mathbf{J}(\mathbf{x}) = \frac{\mathbf{I}(\mathbf{x}) - \mathbf{A}}{r(\mathbf{x})} + \mathbf{A} \tag{2}$$

The dehazed image $\mathbf{J}$ can be restored from the hazy image by estimating the atmospheric light $\mathbf{A}$ and the transmission r. In the next section, we describe how to estimate the atmospheric light and the transmission.

3. PROPOSED METHOD

3.1. Atmospheric Light Estimation

Hazy images can occasionally have un-balanced color due to the scattering effects. This condition may result color distortion in a dehazed image. Therefore, it is customary that a hazy image is processed by white balancing before estimating the atmospheric light. We opted for the *shades-of-gray* color constancy technique [22] due to its simplicity and effectiveness in hazy images [23]. After white balancing, we estimate the atmospheric light which exists in most haze-opaque regions. K. He et al. first pick the top 0.1 percent brightest pixels in the dark channel and selects from them the highest intensity as $\mathbf{A}$ [8]. However, the dark channel can fail to select the most haze-opaque region by the influence of white object. J. Kim et al. estimate $\mathbf{A}$ from quad-tree subdivision by selecting the sub-block which has the largest average value among the four divided blocks from a gray-scaled hazy image repeatedly until pre-specified number of times [9]. Then, $\mathbf{A}$ is selected as an RGB-based color vector minimizing the Euclidean norm with (1, 1, 1) in the finally selected block. However, this method may also fail to estimate $\mathbf{A}$ if an image contains bright regions as shown in Fig. 1(b). To select $\mathbf{A}$ more reliably, we assume that atmospheric light is pervasive over a large portion of hazy image, and its intensity is highest in a local region. By assuming these two aspects of atmospheric light, we estimate $\mathbf{A}$ by quad-tree subdivision using a transformed image as follows. A gray scale image of L, which was obtained from a hazy color image, is subdivided into non-

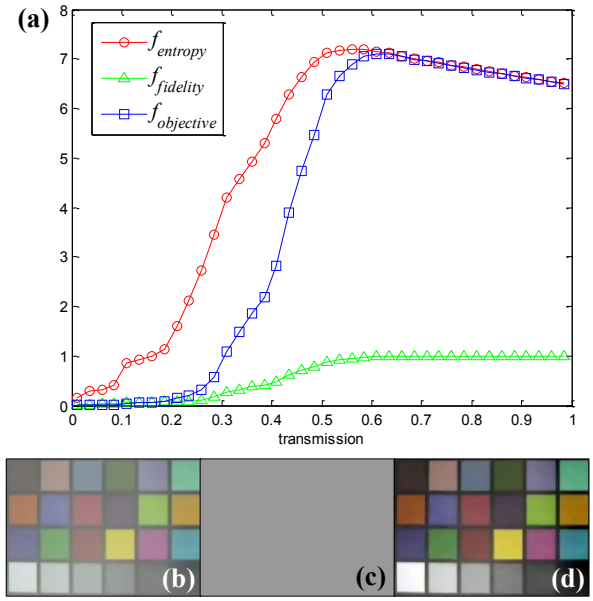

Fig. 3. (a) The graph of the objective function for finding the optimal transmission value. (b) The hazy image. (c) Estimated transmission from the objective function (r = 0.60). (d) Dehazed image using (c) which is the maximum value in blue-line.

overlapping blocks of size $M \times M$. All pixel values in each of these blocks, defined as L_k^{block}, is then then replaced with their minimum value to minimize adverse effects due to bright values of a local object as follows:

$$T_k^{block} = \min_{\mathbf{y} \in L_k^{block}} L(\mathbf{y}), \tag{3}$$

The block size M of 30×30 was set empirically as a tradeoff between accuracy and reliability. Fig. 1(c) shows the transformed image using (3). Since the transformed image T has lower intensity values than original gray scale image L on average, the quad-tree subdivision approach can select the candidate region for estimating the atmospheric light more reliably in the proposed method. This is well illustrated with an example in Fig. 1(c). Note that the proposed method selects sky region as the final candidate region after 5 iterations without being distracted by white floors in bottom regions. Among pixels in the finally selected region, we can estimate the atmospheric light as the color vector of the p-th pixel which minimizes the Euclidean norm, $\| (r_p, g_p, b_p) - (1, 1, 1) \|$. By minimizing the Euclidean nom, we can estimate the atmospheric light more reliably.

3.2. Transmission Estimation

As written in (2), the dehazed image $\mathbf{J}$ depends on transmission r as well as the atmospheric light $\mathbf{A}$. To estimate the transmission which allows the dehazed image to have good contrast while minimizing information loss, we propose the objective function which is comprised of two functions. The first one is the image entropy $f_{entropy}$ as a contrast measure. It has been proven to be a powerful tool for image processing and a statistical measure of randomness that can be used to characterize texture of an image [16, 20]. Note that the entropy of haze-free image is bigger than that of hazy image at same scene, since the haze-free image is

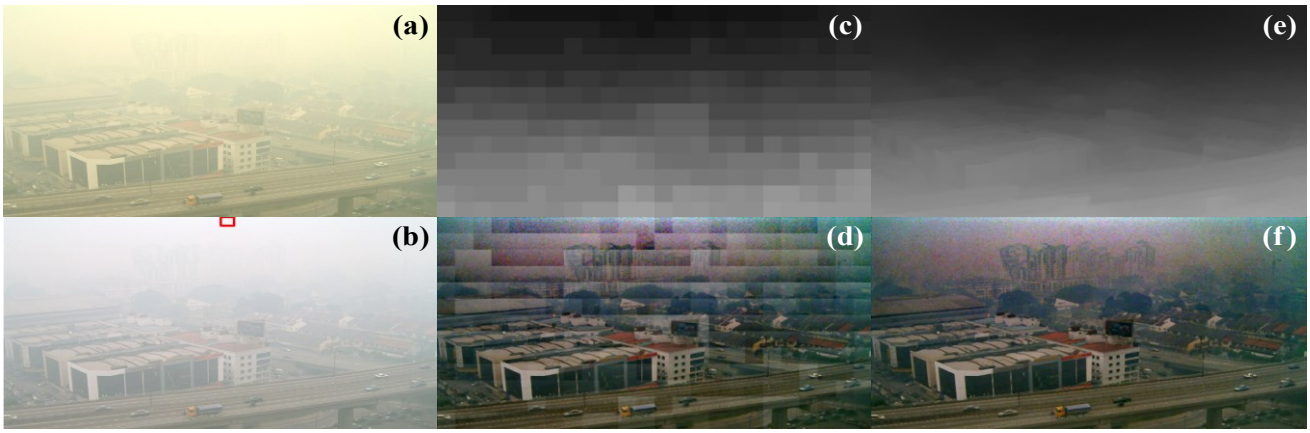

Fig. 4. Dehazing procedure of the proposed method. (a) Hazy image. (b) White balance image (The red rectangle is the final selected block by the proposed method). (c) Estimated optimal transmission from (8). (d) Dehazed image using (c). (e) Refined transmission. (f) Dehazed image using (e).

distributed more randomly compared to hazy image. An image entropy can be expressed by the function of transmission r as follows:

$$f_{entropy}(r) = -\sum_{i=0}^{255} \frac{h_i(r)}{N} \log \frac{h_i(r)}{N}, \tag{4}$$

where N is the number of pixels in the image, $h_i(r)$ is the number of pixels that have intensity i in the gray-scaled image of **J** calculated from (2), when the transmission is set to r. However, the dehazed image may take values smaller than 0 or larger than 255 when (**I**(**x**) – **A**) term in (2) is divided by small value of r. In such a case, those underflow and overflow values are required to be truncated. However, an excessive number of truncations leads to misestimation of transmission and results in color distortion in the dehazed image as shown in red circles of Fig. 2(b). Therefore, we define the second function $f_{fidelity}$ as an information fidelity measure to provide more faithful dehazing results and reduce the overflow and underflow when we estimate the transmission. $f_{fidelity}(r)$ is defined as follows:

$$f_{fidelity}(r) = \min_{c\in\{r,g,b\}} s^c(r), \tag{5}$$

$$s^c(r) = \frac{1}{N}\sum_{p=1}^{N}\delta(p), \quad \delta(p) = \begin{cases} 1, & 0 \le J^c(p) \le 255 \\ 0, & otherwise \end{cases} \tag{6}$$

where, $s^c(r)$ expresses the ratio of pixels between 0 and 255 at each color channel of the dehazed image **J** when the transmission is set to r. That is, $f_{fidelity}(r)$ is the minimum ratio of the number of pixels which are not truncated among the RGB color channels in **J**. Note that as the number of truncated pixels becomes fewer, $f_{fidelity}(r)$ becomes larger. In other words, we can restrict the amount of truncation effectively by maximizing the proposed information fidelity measure. Consequently, the proposed objective function is defined as a product of two measures:

$$f_{objective}(r) = f_{entropy}(r) \cdot f_{fidelity}(r), \tag{7}$$

By maximizing the objective function in (7), we can estimate the transmission which provides good contrast and faithful dehazing results without distortions as shown in Fig. 2(c). In Fig. 3(a), red line and green line show the variation of entropy measure in (4) and information fidelity measure in (5), respectively, according to r at a homogeneous haze condition as shown in Fig. 3(b). Blue line in Fig. 3(a) shows the variation of $f_{objective}(r)$. In this example, when r becomes smaller than about 0.6, $f_{objective}(r)$ becomes smaller due to the truncation loss. That is, as the truncated values are increased, $f_{entropy}$ and $f_{fidelity}$ are decreased since the more pixels are outside the range and concentrated to 0 and 255. Note that when r exceeds about 0.6, the $f_{fidelity}$ approaches to 1, which means that no pixels are truncated. However, $f_{entropy}$ starts to decrease when r approaches to 1. This is because the degree of dehazing operation gets smaller in (2), i.e., **J**(**x**) ≈ **I**(**x**). Remember that the entropy of hazy image is smaller than that of haze-free image at same scene. Thus the resultant $f_{objective}(r)$ has a concave shape as shown in Fig. 3(a) and the optimal transmission can be determined by maximizing $f_{objective}$ roughly between 0.5 and 0.7 in this example. Therefore, we determine the transmission r to maximize the objective function $f_{objective}(r)$.

However, since the values of the transmission in outdoor hazy image is non-homogeneous and space-varying [6]-[9], local optimal transmission is estimated at each of the non-overlapped sub-block regions as follows:

$$r_k^{block} = \arg\max_{r\in\{0.01\le r\le 1\}} f_{objective}(r), \tag{8}$$

where r_k^{block} is the k-th sub-block which is divided by pre-specified block size from a hazy image. If the block size is too big or too small, estimated transmission is likely to be inaccurate. More specifically, if the block size is too big, it may encompass regions supposed to have different transmission values. On the contrary, if the block is too small, estimated transmission may not be exact due to the insufficient number of pixels. We set the block size to 30×30 experimentally in this paper. The minimum transmission value is set by 0.01 to prevent division by zero in (2). Fig. 4(c) shows the estimated transmission values for each blocks in (8).

3.3. Transmission Refinement

Since the transmission from (8) is estimated in non-overlapping manner for each sub-block, block artifacts can occur at the dehazed

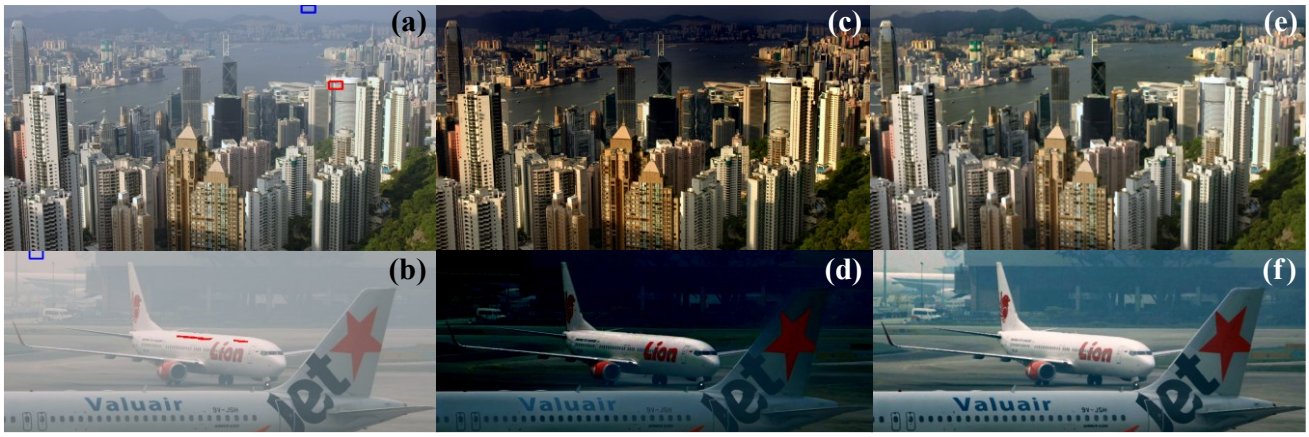

Fig. 5. The comparison of the proposed method with conventional methods. (a) Hazy image (The red rectangle is the final selected block to determine the atmospheric light by conventional work [9]). (b) Hazy image (The red area in upper side of airplane "Lion" represents the top 0.1% of the brightest pixels in dark channel, in which the biggest pixel value is selected as the atmospheric light [8]). (c) Dehazed image by Kim's work [9]. (d) Dehazed image by He's work [8]. (e), (f) Dehazed images by proposed method. The blue rectangles in (a) and (b) are finally selected block to determine the atmospheric light by proposed method.

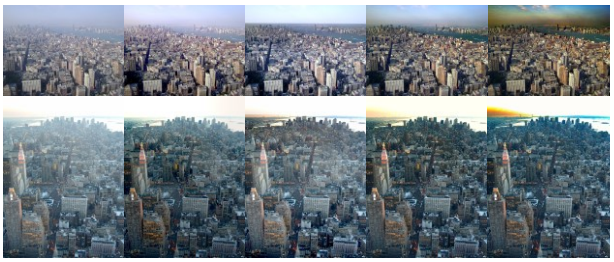

(a) (b) (c) (d) (e)

Fig. 6. The comparison with other methods. (a) Hazy image. (b) Fattal's work [6]. (c) Kopf's work [19]. (d) He's work [8]. (e) Proposed method.

image as depicted in Fig. 4(d). To alleviate those artifacts, we employ our previous work in [10] which refines the transmission by WLS optimization solution [17]. We set the smoothing parameter λ to 0.8 and sensitivity parameter α to 1.2, respectively. Fig. 4(e) shows the refined transmission by WLS optimization solution.

4. EXPERIMENTAL RESULTS

To validate effectiveness of the proposed method, we compared our method with conventional methods [6, 8, 9, 19]. Fig. 5 shows the comparison of the proposed method with Kim's method [9] and He's method [8]. As apparent in Fig. 5(a) and (b), the proposed method estimates the atmospheric light more reliably compared to the conventional methods [8, 9]. Consequently, the proposed method provides more visually pleasing results compared to the conventional methods as shown in Fig. 5(e) and (f).

We also compared performance of the proposed method with other conventional methods whose results were uploaded on webpages [25] in terms of Colorfulness [24], Global Contrast Factor (GCF) [21] measure and visible edge gradient method [18]. The visible edge gradient [18] which consists of three indicators e, r, σ is a method for measuring visibility using the input hazy image and the restored image. e is the rate of edges newly visible after restoration, and r is the mean ratio of the gradient norms at visible edges. σ is the percentage of pixels that becomes completely black or completely white after restoration. We should inform that dehazed image has better quality as σ becomes smaller and the other indicators become bigger. The quantitative results are shown in Table 1, and Table 2. Fattal's method represents good performance in close-range regions. However, their method dose not remove haze effectively in far-range regions. While Kopf's method shows good scores in GCF and r, it is less effective in terms of Colorfulness and σ. While Kopf's method and He's method show limited performance since they have good scores only in GCF and σ. The proposed method shows better performance qualitatively as well as quantitatively overall.

Table 1. Quantitative measurements of the 1st row in Fig. 6.

Index	Fattal	Kopf	He	Proposed
e [18]	0.1059	0.0168	0.0234	**0.3213**
r [18]	1.5335	1.6136	1.6286	**2.2744**
σ [18]	1.6988	1.3598	**0.0136**	0.0672
Colorfulness	652.45	455.84	963.62	**1127.42**
GCF	7.87	8.53	**8.63**	8.49

Table 2. Quantitative measurements of the 2nd row in Fig. 6.

Index	Fattal	Kopf	He	Proposed
e [18]	0.0538	0.03607	0.04821	**0.0849**
r [18]	1.2875	1.4091	1.3979	**1.4114**
σ [18]	9.4053	0.2993	**0.0056**	0.0574
Colorfulness	387.01	390.67	509.90	**706.09**
GCF	5.89	6.65	6.72	**6.80**

5. CONCLUSIONS

In this paper, we proposed an effective single image dehazing algorithm. The proposed method estimates the atmospheric light by quad-tree subdivision using transformed image after white balance processing. Then, the optimal transmission is estimated by maximizing the objective function that consists of image entropy and information fidelity. Finally, the transmission is refined by WLS optimization procedure. From the limited set of experiments, it successfully enhanced image contrast while retaining color fidelity.

6. REFERENCES

[1] J.P. Oakley and B.L. Satherley, "Improving image quality in poor visibility conditions using a physical model for contrast degradation," *IEEE Transactions on Image Processing*, vol.7, no.2, pp. 167-179, Feb 1998.

[2] S.G. Narasimhan and S.K. Nayar, "Contrast restoration of weather degraded images," *IEEE Transactions on Pattern Analysis and Machine Intelligence*, vol.25, no. 6, pp. 713-724, June 2003.

[3] D. Kim, C. Jeon, B. Kang, H. Ko, "Enhancement of Image Degraded by Fog Using Cost Function Based on Human Visual Model", *IEEE International Conference on Multisensor Fusion and Integration for Intelligent Systems (MFI)*, pp. 64-67, Aug. 2008.

[4] S.K. Nayar, S.G. Narasimhan, "Interactive (De)Weathering of an Image using Physical Models," *Proceedings of ICCV Workshop on Color and Photometric Methods in Computer Vision*, Oct. 2003.

[5] J. P. Oakley and H. Bu, "Correction of simple contrast loss in colorimages," *IEEE Transactions on Image Processing*, vol. 16, no. 2, pp.511–522, 2007.

[6] R. Fattal, "Single image dehazing," *Proc. of ACM SIGGRAPH '08*, 2008.

[7] R. Tan, "Visibility in bad weather from a single image," *IEEE conference on Computer Vision and Pattern Recognition* (*CVPR*), pp. 1-8, June 2008.

[8] K. He, J. Sun, X. Tang, "Single Image Haze Removal Using Dark Channel Prior," *IEEE Transactions on Pattern Analysis and Machine Intelligence*, vol. 33, no. 12, pp. 2341-2353, Dec. 2011.

[9] J.H. Kim, J.Y. Sim, C.S. Kim, "Single image dehazing based on contrast enhancement," *2011 IEEE International Conference on Acoustics, Speech and Signal Processing* (*ICASSP*), pp. 1273-1276, May 2011.

[10] D.B. Park, David K, Han, H.S. Ko, "Single Image Haze Removal With WLS-based Edge-preserving Smoothing Filter" *2013 IEEE International Conference on Acoustics, Speech and Signal Processing* (*ICASSP*), pp. 2469-2473, May 2013.

[11] Y.Y. Schechner, S.G. Narasimhan and S.K. Nayar, "Instant dehazing of images using polarization," *Proceedings of the 2001 IEEE Computer Society Conference on Computer Vision and Pattern Recognition. (CVPR)*, vol.1, pp. 325-332, 2001.

[12] S.K. Nayar, S.G. Narasimhan. "Vision in Bad Weather," *The Proceedings of the Seventh IEEE International Conference on Computer Vision*, vol. 2, pp. 820-827, Sept. 1999.

[13] Yuhui Zhu, Bin Fang, Huiqing Zhang. "Image De-Weathering for Road Based on Physical Model," *International Conference on Information Engineering and Computer Science 2009*, Wuhan, China, Dec. 2009

[14] W.Middleton, "*Vision through the Atmosphere*", University of Toronto Press, 1952.

[15] Nicolas Hautiere, Didier Aubert. "Contrast Restoration of Foggy Images through use of an Onboard Camera," *Proceedings of the 8th International IEEE Conference on Intelligent Transportation Systems*, Vienna, Austria, Sept. 2005.

[16] G. Deng "An Entropy Interpretation of the Logarithmic Image Processing Model With Application to Contrast Enhancement," *IEEE Transactions on Image Processing*, vol. 18, issue 5, pp. 1135-1140, May 2009.

[17] Z. Farbman, R. Fattal, D. Lischinski, and R. Szeliski, "Edge-preserving decomposition for multi-scale tone and detail manipulation," *ACM Transactions on Graphics*, vol. 27, issue 3, no. 67, Aug. 2008.

[18] N. Hautiere, J. P. Tarel, D. Aubert, and E. Dumont, "Blind contrast enhancement assessment by gradient ratioing at visible edges," *Image Analysis & Stereology Journal*, 27(2):87-95, June 2008.

[19] J. Kopf, B. Neubert, B. Chen, M. Cohen, D. Cohen-Or, O. Deussen, M. Uyttendaele, and D. Lischinski, "Deep photo: Model-based photograph enhancement and viewing," *ACM Trans. Graph.*, vol. 27, no. 5, pp. 1–10, Dec. 2008.

[20] S.F. Gull, J. Skilling, "Maximum entropy method in image processing," *IEE Proceedings Communications, Radar and Signal Processing*, vol. 131, issue 6, pp. 646-659, Oct. 1984.

[21] Kresimir Matkovic et al., "Global Contrast Factor –a New Approach to Image Contrast," *Proceedings of the First Eurographics conference on Computational Aesthetics in Graphics, Visualization and Imaging*, pp. 159-167, May 2005

[22] G. Finlayson and E. Trezzi, "Shades of gray and colour constancy," *in Proc. 12th Color Imag. Conf.*, pp. 37–41, 2004.

[23] C.O. Ancuti, C. Ancuti, "Single image dehazing by multi-scale fusion," *IEEE Transactions on Image Processing*, vol. 22, issue 8, pp. 3271-3282. Aug. 2013.

[24] S. Susstrunk, S. Winkler, "Color image quality on the Internet," *Proc. IS&T/SPIE Electronic Imaging 2004*: *Internet Imaging V*, vol. 5304, pp.118-131, 2004.

[25] http://perso.lcpc.fr/tarel.jean-philippe/visibility/